Epidermal Growth Factor Receptor Inhibition Modulates the Nuclear Localization and Cytotoxicity of the Auger Electron–Emitting Radiopharmaceutical 111In-DTPA–Human Epidermal Growth Factor

Kristy E. Bailey[1,2], Danny L. Costantini[3,4], Zhongli Cai[2], Deborah A. Scollard[4], Zhuo Chen[2], Raymond M. Reilly[3,4], and Katherine A. Vallis[1,2,5]

[1]Department of Medical Biophysics, University of Toronto, Toronto, Ontario, Canada; [2]Division of Applied Molecular Oncology, Ontario Cancer Institute/Princess Margaret Hospital, University Health Network, Toronto, Ontario, Canada; [3]Leslie Dan Faculty of Pharmacy, University of Toronto, Toronto, Ontario, Canada; [4]Division of Nuclear Medicine, Toronto General Hospital Research Institute, Toronto, Ontario, Canada; and [5]Radiation Medicine Program, Princess Margaret Hospital, University Health Network, Toronto, Ontario, Canada

111In-DTPA–human epidermal growth factor (111In-DTPA-hEGF [DTPA is diethylenetriaminepentaacetic acid]) is an Auger electron–emitting radiopharmaceutical that targets EGF receptor (EGFR)–positive cancer. The purpose of this study was to determine the effect of EGFR inhibition by gefitinib on the internalization, nuclear translocation, and cytotoxicity of 111In-DTPA-hEGF in EGFR-overexpressing MDA-MB-468 human breast cancer cells. **Methods:** Western blot analysis was used to determine the optimum concentration of gefitinib to abolish EGFR activation. Internalization and nuclear translocation of fluorescein isothiocyanate–labeled hEGF were evaluated by confocal microscopy in MDA-MB-468 cells (1.3×10^6 EGFRs/cell) in the presence or absence of 1 μM gefitinib. The proportion of radioactivity partitioning into the cytoplasm and nucleus of MDA-MB-468 cells after incubation with 111In-DTPA-hEGF for 24 h at 37°C in the presence or absence of 1 μM gefitinib was measured by cell fractionation. DNA double-strand breaks caused by 111In were quantified using the γ-H2AX assay, and radiation-absorbed doses were estimated. Clonogenic survival assays were used to measure the cytotoxicity of 111In-DTPA-hEGF alone or in combination with gefitinib. **Results:** Gefitinib (1 μM) completely abolished EGFR phosphorylation in MDA-MB-468 cells. Internalization and nuclear translocation of fluorescein isothiocyanate–labeled EGF were not diminished in gefitinib-treated cells compared with controls. The proportion of internalized 111In that localized in the nucleus was statistically significantly greater when 111In-DTPA-hEGF was combined with gefitinib compared with 111In-DTPA-hEGF alone (mean $\pm$ SD: 26.0% $\pm$ 5.5% vs. 14.6% $\pm$ 4.0%, respectively; $P < 0.05$). Induction of γ-H2AX foci was greater in MDA-MB-468 cells that were treated with 111In-DTPA-hEGF (250 ng/mL, 1.5 MBq/mL) plus gefitinib (1 μM) compared with those treated with 111In-DTPA-hEGF alone (mean $\pm$ SD: 35 $\pm$ 4 vs. 24 $\pm$ 5 foci per nucleus, respectively). In clonogenic assays, a significant reduction in the surviving fraction was observed when 111In-DTPA-hEGF (5 ng/mL, 6 MBq/μg) was combined with gefitinib (1 μM) compared with 111In-DTPA-hEGF alone (42.9% $\pm$ 5.7% vs. 22.9% $\pm$ 3.6%, respectively; $P < 0.01$). **Conclusion:** The efficacy of 111In-DTPA-hEGF depends on internalization and nuclear uptake of the radionuclide. Nuclear uptake, DNA damage, and cytotoxicity are enhanced when 111In-DTPA-hEGF is combined with gefitinib. These results suggest a potential therapeutic role for peptide receptor radionuclide therapy in combination with tyrosine kinase inhibitors.

Key Words: targeted radiotherapy; Auger electrons; 111In-DTPA-hEGF; EGFR inhibition; nuclear localization

The human epidermal growth factor receptor (EGFR) is a transmembrane tyrosine kinase receptor that transmits signals that control cell growth, migration, and proliferation. Ligand-dependent activation of EGFR leads to dimerization and autophosphorylation of the receptor and subsequent activation of downstream molecules involved in mitogenic signaling (1). EGFR overexpression occurs in 30%–60% of breast carcinomas and is associated with hormone resistance and a poor prognosis (2).

Inhibition of the EGFR has been explored extensively as a promising approach to the treatment of cancer in recent years. Several drugs that block EGFR activation or function

have been developed and used as single agents or in combination with other treatments (3). An important group of compounds blocks ligand-induced activation of EGFR tyrosine kinase. Gefitinib (Iressa, ZD1839; AstraZeneca), for example, is an orally active tyrosine kinase inhibitor (TKI) that targets the adenosine triphosphate–binding site in the cytoplasmic domain of EGFR (4). Gefitinib has shown efficacy in several solid tumors, including head and neck and non–small cell lung cancer, and clinical trials are being conducted to define the role of gefitinib in the management of these cancers (5). Gefitnib has shown only limited benefit as a single agent in the treatment of metastatic breast cancer (6). However, trials of gefitinib in combination with trastuzumab or chemotherapy are being conducted (7,8). Preclinical studies also suggest synergistic effects of gefitinib in combination with hormonal agents (9).

Ionizing radiation causes EGFR phosphorylation and activation, and an inverse correlation exists between EGFR expression level and radiosensitivity in some tumors (10). In vitro studies have demonstrated synergy between EGFR inhibition and radiation, and this phenomenon is also evident in animal xenograft models (11). These early observations led to the development of clinical protocols that combine radiation with EGFR inhibition. For example, a recently reported phase III trial has confirmed the efficacy of EGFR inhibition in combination with radiation therapy in the treatment of advanced head and neck cancer (12). The molecular mechanisms that are thought to account for radiosensitization by EGFR inhibition include prevention of tumor cell proliferation and repopulation, disruption of normal cell cycle control, and interference with repair of radiation-induced DNA damage (13).

[111]In-Labeled human epidermal growth factor (^{111}In-DTPA-hEGF [DTPA is diethylenetriaminepentaacetic acid]) is a radiopharmaceutical that binds the EGFR, is rapidly internalized, and translocates to the nucleus (14). [111]In emits densely ionizing Auger electrons, 99% of which have a range of <1 μm in tissue and which are highly damaging to DNA (15). On a molar concentration basis, ^{111}In-DTPA-hEGF was found to be 85-, 200-, and 300-fold more effective at inhibiting the growth of the EGFR-positive human breast cancer cell line MDA-MB-468 than paclitaxel, methotrexate, and doxorubicin, respectively (16). ^{111}In-DTPA-hEGF was also found to exert a strong antitumor effect on MDA-MB-468 xenografts in athymic mice (17). Although these results demonstrate a potent anticancer effect of ^{111}In-DTPA-hEGF, it is possible that the radiotoxicity of ^{111}In-DTPA-hEGF might be partially attenuated by activation of the EGFR by the EGF moiety of the drug. To explore this, ^{111}In-DTPA-hEGF was combined with inhibition of the tyrosine kinase function of the receptor using gefitinib. Gefitinib was selected for this purpose because it was shown previously to enhance binding and cellular uptake of astatinated and iodinated EGF in some cell lines (18,19). Strategies that increase the internalization and then nuclear translocation of ^{111}In-DTPA-hEGF are likely to enhance the cytotoxicity of this agent because of the ultrashort range of the Auger electrons.

Our findings indicate that concurrent gefitinib increases the nuclear uptake of ^{111}In-DTPA-hEGF, resulting in a greater level of DNA damage and enhanced cytotoxicity compared with ^{111}In-DTPA-hEGF alone. These observations suggest that combining Auger electron–emitting radiopharmaceuticals that target peptide receptors with small-molecule TKIs may be a useful therapeutic strategy.

MATERIALS AND METHODS

Cell Culture

MDA-MB-468 human breast cancer cells were obtained from the American Type Culture Collection and were cultured in Dulbecco's minimum essential medium ([DMEM] Ontario Cancer Institute) containing penicillin (100 units/mL), streptomycin (100 μg/mL), and L-glutamine (2 mM) and supplemented with 10% fetal calf serum.

Radiopharmaceutical Synthesis

hEGF (Upstate Biotechnology) was derivatized with DTPA and labeled to high specific activity (3–6 MBq/μg) with ^{111}In-acetate as previously described (20). The radiochemical purity of ^{111}In-DTPA-hEGF was 95%–98%, as determined by silica-gel instant thin-layer chromatography in 100 mM sodium citrate, pH 5.

Effect of Gefitinib on EGFR Signaling in MDA-MB-468 Cells

To determine the concentration of gefitinib required to inhibit EGFR phosphorylation, MDA-MB-468 cells were cultured in serum-free DMEM for 3 h. Gefitinib was added in a range of concentrations (0–1 μM) for 3 h, and 20 ng/mL hEGF (Upstate Biotechnology) was added for the last 15 min before cells were harvested. Cells were washed in ice-cold phosphate-buffered saline (PBS) and lysed in NTEN buffer (150 mM sodium chloride, 20 mM Tris, pH 8.0, 1.0 mM EDTA [ethylenediaminetetraacetic acid], 0.5% Nonidet P-40 [NP-40; BDH Chemicals]) containing complete mini-EDTA–free protease inhibitor cocktail tablets (Roche Diagnostics). Lysates were resolved by NaDodSO$_4$–polyacrylamide gel electrophoresis. Proteins were transferred to Immobilon-P transfer membrane (Millipore), blocked with 10% nonfat dried milk in Tris-buffered saline with Tween 20, and probed with anti-EGFR (clone 13, 1:1,000; BD Transduction Laboratories), antiphospho-EGFR (clone 9H2, 1:1,000; Calbiochem), anti-MAPK (1:200; Cell Signaling Technology), antiphospho-MAPK (Thr-202/Tyr-204, 1:100; Cell Signaling Technology), anti-SAPK/JNK (1:200; Cell Signaling Technology), antiphospho-SAPK/JNK (Thr-183/Tyr-185, 1:100; Cell Signaling Technologies), anti-p38 (Cell Signaling Technology), or antiphospho-p38 (Thr-180/Tyr-182, 1:100; Cell Signaling Technology) antibodies at 4°C overnight. After washing 3 times, primary antibodies were detected with horseradish peroxidase–conjugated antimouse or antirabbit secondary antibody as appropriate (Perkin Elmer Life Sciences). Bands were visualized using enhanced chemiluminescence (Super Signal West Pico Chemiluminescent).

Effect of Gefitinib on Internalization and Distribution of EGF and ^{111}In-DTPA-hEGF in MDA-MB-468 Cells

Fluorescein isothiocyanate was conjugated to hEGF as described (21). Fluorescein-hEGF was separated from free fluorescein by size-exclusion chromatography on a P-2 minicolumn

(Bio-Rad Laboratories) eluted with 150 mM sterile sodium chloride, pH 7.4. MDA-MB-468 cells (1×10^3) were plated on 8-well chamber slides (Nunclon; Canadian Life Technologies) and cultured for 24 h at 37°C in DMEM. Gefitinib (1 μM) was added for an additional 3 h or cells were left untreated (controls). Cells were washed 3 times with PBS and incubated for 1 h with 100 nM fluorescein-hEGF (with or without 1 μM gefitinib) in 150 mM sterile sodium chloride, pH 7.4. Cells were rinsed with 150 mM sodium chloride, pH 7.4, and fixed with 3.7% paraformaldehyde. After another 3 rinses with 150 mM sodium chloride, pH 7.4, slides were mounted with Vectashield mounting media (Vector Laboratories) containing the nuclear stain DAPI (4′,6′-diamidino-2-phenylindole dihydrochloride) and allowed to dry overnight at 4°C. The intracellular localization of fluorescein-hEGF (λ_{excit}, 470–490 nm) and DAPI (λ_{excit}, 340–380 nm) was evaluated using a Zeiss LSM 510 confocal laser-scanning microscope. Images were obtained of 1-μm slices and processed using Adobe Photoshop 7.0.

To determine the effect of gefitinib on the intracellular distribution of ^{111}In-DTPA-hEGF, MDA-MB-468 cells (3×10^6) were incubated in medium with or without gefitinib (1 μM) in 6-well culture dishes for 3 h, which was followed by the addition of ^{111}In-DTPA-hEGF (5 ng/mL, 3.7 MBq/μg) for 24 h. The 24-h time point was chosen as we have shown previously that nuclear accumulation of ^{111}In-DTPA-hEGF increases for up to 24 h in MDA-MB-468 cells (14). After 24 h, unbound radioactivity was collected by transferring cell suspensions to tubes and recovering the medium by centrifugation at 600g for 10 min. This medium was combined with rinses obtained by resuspending the cells 3 times in PBS and centrifugation. The cells were then resuspended in 1 mL of 200 mM sodium acetate/500 mM sodium chloride, pH 2.5, for 5 min at 4°C to remove cell-surface–bound radioactivity. This acidic wash was recovered by centrifugation. The cells were rinsed 3 times with PBS, and the acidic wash and PBS were combined. Cells were then lysed and separated into cytoplasmic and nuclear fractions. In brief, cells were incubated with 1 mL of lysis buffer (25 mM KCl, 5 mM $MgCl_2$, 10 mM Tris-HCl, pH 8.0, 1 mM dithiothreitol, 0.5% NP-40 plus protease inhibitor cocktail tablets) for 15 min at 4°C. Cell lysates were centrifuged at 1,000g for 5 min, and the supernatant was collected. The pellet was rinsed 3 times in PBS and each rinse was collected by centrifugation. The supernatant and the 3 rinses contained the cytoplasmic radioactivity. The cell pellet was incubated at 4°C for 15 min with nucleus isolation buffer (500 mM sodium chloride, 10 mM Tris-HCl, pH 8.0, 5 mM EDTA, 0.1% NP-40 with protease inhibitors). Vigorous pipeting and vortexing were used to break open the nuclear membrane. Samples were centrifuged at 12,000g for 15 min, and the supernatant was collected. The pellet was rinsed 3 times with PBS and centrifuged for 5 min at 10,000g. The supernatant and the 3 washes contained the nuclear radioactivity. The radioactivity in the 4 fractions (unbound, surface-bound, cytoplasmic, and nuclear) was measured using a γ-counter (Auto Gamma model 5650; Packard Instruments).

DNA Damage in MDA-MB-468 Cells Evaluated Using γ-H2AX Assay

Subconfluent MDA-MB-468 cells were harvested by trypsinization, seeded onto sterilized cover glasses (22×22 mm, Fisherfinest; Fisher Scientific), and placed in 6-well tissue culture plates (10^5 cells/well) in 1 mL of DMEM. After 24 h, the cells were incubated with DTPA-hEGF (250 ng/mL), ^{111}In-acetate

(1.5 MBq/mL), gefitinib (1 μM), ^{111}In-DTPA-hEGF (250 ng/mL, 1.5 MBq/mL), or gefitinib plus ^{111}In-DTPA-hEGF in 1 mL of fresh DMEM for 20 h. Cells treated with gefitinib plus ^{111}In-DTPA-hEGF or gefitinib alone had been pretreated with 1 μM gefitinib for 3 h. Control dishes were incubated with medium alone.

After incubation, cells were rinsed with PBS and fixed with 2% paraformaldehyde plus 0.5% Triton X-100/PBS, pH 8.2, for 15 min, permeabilized with PBS containing 0.5% NP-40 for 15 min, and blocked in 2% bovine serum albumin (BSA) plus 1% donkey serum-PBS for at least 1 h. Cells were then incubated with mouse monoclonal anti-γ-H2AX antibody (1:800; Upstate Biotechnology) in 3% BSA-PBS overnight at 4°C and then incubated with Alexa Fluor 488 donkey antimouse secondary antibody (1:500; Invitrogen) for 45 min at room temperature. Finally, cells were stained with DAPI (0.2 μg/mL) for 5 min. After each of these steps, cells were rinsed in PBS twice for 5 min, except that after incubation with antibodies, cells were rinsed 3 times with 0.5% BSA plus 0.175% Tween-20/PBS for 10 min. The cover glasses were removed and mounted on microscope slides (Fisherbrand) using Vectashield Mounting Medium (Vector Laboratories). From the step using the secondary antibody, all procedures were performed in the dark. The cover glasses were wrapped with aluminum foil and stored at 4°C for later image acquisition.

The images of γ-H2AX foci and nuclei were obtained using a Zeiss LSM 510 confocal microscope. Optical sections (1.2 μm) through the thickness of the cells were imaged and combined in a z-projection. The projected images were processed using ImageJ (U.S. National Institutes of Health). At least 30 cells were imaged and analyzed for each data point in each experiment.

Clonogenic Survival Assays

MDA-MB-468 cells were treated with ^{111}In-DTPA-hEGF (5–250 ng/mL; 6 MBq/μg) or unlabeled DTPA-hEGF (250 ng/mL) in medium with or without 1 μM gefitinib. Cells exposed to 1 μM gefitinib plus ^{111}In-DTPA-hEGF were pretreated with 1 μM gefitinib for 3 h. Control dishes were incubated with medium with or without 1 μM gefitinib. All dishes were incubated at 37°C for 24 h. Cells were washed with PBS, trypsinized, and resuspended in medium. Cells were seeded in 6-well dishes for 10 d at 37°C to allow colony formation. Cultures were rinsed with PBS and stained with methylene blue (1% in a 1:1 mixture of ethanol and water). The number of colonies (>50 cells) in each dish was counted under light microscopy. The plating efficiency was determined by dividing the number of colonies formed in the untreated control dishes by the number of cells seeded. The surviving fraction (SF) was calculated by dividing the number of colonies formed by the number of cells seeded multiplied by the plating efficiency.

RESULTS

Effect of Gefitinib on EGFR Signaling in MDA-MB-468 Cells

The treatment of cells with hEGF (20 ng/mL) for 15 min resulted in a marked increase in EGFR phosphorylation (Fig. 1A). The phosphorylation status of EGFR was reduced in cells pretreated for 3 h with gefitinib (0.1–0.5 μM). Gefitinib at a concentration of 1 μM completely blocked EGF-induced phosphorylation of EGFR. Phosphorylation of the downstream targets of EGFR (MAPK, SAPK/JNK, and p38) was also inhibited by 1 μM gefitinib
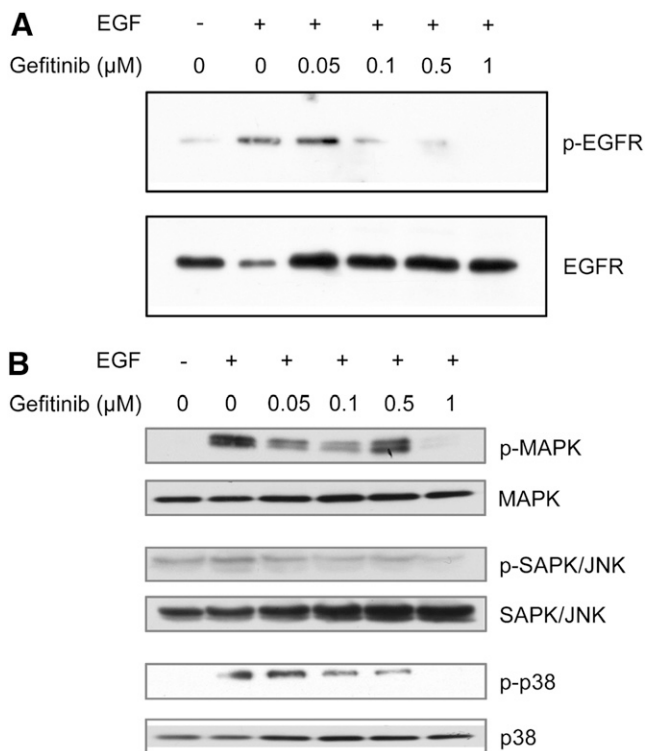
FIGURE 1. EGF-induced EGFR phosphorylation and activation is blocked by 1 μM gefitinib in MDA-MB-468 cells. Western blot analyses of MDA-MB-468 cells without (−) or stimulated with 20 ng/mL EGF (+) for 15 min, following incubation with 0.05–1 μM gefitinib for 3 h at 37°C. (A) Total protein samples were probed with antiphospho-EGFR Tyr-1173 and anti-EGFR antibodies. (B) Anti-MAPK, antiphospho-MAPK (p42/p44), anti-SAPK/JNK, antiphospho-SAPK/JNK, anti-p38, and antiphospho-p38 antibodies were used to determine phosphorylation status of downstream proteins in EGFR signaling cascade. Phosphorylation of EGFR and activation of downstream proteins was completely blocked by 1 μM gefitinib.

(Fig. 1B). This concentration of gefitinib was selected for use in subsequent nuclear localization and clonogenic survival experiments.

Effect of Gefitinib on Internalization and Distribution of EGF and ^{111}In-DTPA-hEGF in MDA-MB-468 Cells

Using confocal microscopy it was found that after 1 h, fluorescein-hEGF was present in both the cytoplasm and the nuclei in the presence and absence of gefitinib, as indicated by the superimposition of green (EGF) on blue (DAPI) staining (Fig. 2). There was no significant difference in the proportion of radioactivity that bound to the cell surface or internalized after 24 h when MDA-MB-468 cells were exposed to ^{111}In-DTPA-hEGF plus gefitinib compared with ^{111}In-DTPA-hEGF alone. However, when cells were treated with ^{111}In-DTPA-hEGF plus 1 μM gefitinib, there was a change in the distribution of radioactivity within the cell, with a significantly greater proportion localized to the nucleus and less in the cytoplasm compared with ^{111}In-DTPA-hEGF alone (Table 1). The combination of gefitinib and ^{111}In-DTPA-hEGF resulted in an almost 2-fold increase

in radioactivity in the nuclear fraction compared with ^{111}In-DTPA-hEGF alone (expressed as a percentage of internalized ^{111}In-DTPA-hEGF: 26.0% ± 5.5% vs. 14.6% ± 4.0%, respectively; $P < 0.05$).

DNA Damage in MDA-MB-468 Cells Evaluated Using γ-H2AX Assay

Cells exposed to gefitinib plus ^{111}In-DTPA-hEGF showed a statistically significant increase in the mean number of γ-H2AX foci per nucleus compared with control untreated cells (35.4 ± 4.2 vs. 6.3 ± 1.3 foci, respectively; $P < 0.001$) (Fig. 3). There was a 1.5-fold increase in the mean number of γ-H2AX foci in cells exposed to the combination treatment compared with ^{111}In-DTPA-hEGF alone, and this was statistically significant (35.4 ± 4.2 vs. 23.8 ± 5.2 foci, respectively; $P < 0.05$). These results indicate that the enhancement of nuclear translocation of ^{111}In-DTPA-hEGF in the presence of gefitinib is associated with an increase in DNA double-strand breaks (DNA-dsbs).

DTPA-hEGF and gefitinib alone did not cause a statistically significant increase in the number of γ-H2AX foci compared with control untreated cells ($P = 0.10$ and 0.06, respectively). ^{111}In-Acetate alone caused an increase in the number of γ-H2AX foci compared with control (13.6 ± 2.5 vs. 6.3 ± 1.3 foci, respectively; $P < 0.05$) (Fig. 3). ^{111}In-DTPA-hEGF, however, resulted in a significantly greater number of foci compared with ^{111}In-acetate alone (23.8 ± 5.2 vs. 13.6 ± 2.5 foci, respectively; $P < 0.05$).

Clonogenic Survival Assays

The SF of MDA-MB-468 cells was significantly lower when cells were treated with 1 μM gefitinib plus ^{111}In-DTPA-hEGF (5–150 ng/mL, 6 MBq/μg) compared with ^{111}In-DTPA-hEGF alone. For example, the SF of cells treated with 5 ng/mL ^{111}In-DTPA-hEGF was 42.9% ± 5.7%, whereas the SF of cells exposed to ^{111}In-DTPA-hEGF (5 ng/mL) plus gefitinib was 22.9% ± 3.6% ($P < 0.01$). At the highest concentration of ^{111}In-DTPA-hEGF tested, 250 ng/mL (6 MBq/μg), the SF was reduced to 6%, and the addition of gefitinib was not associated with a further reduction in the SF (Fig. 4). Unlabeled DTPA-hEGF (250 ng/mL) alone resulted in a modest reduction in SF (60.6% ± 9.9%). This is consistent with the reported observation that high concentrations of EGF are inhibitory to the growth of MDA-MB-468 cells (16). The same concentration of ^{111}In-DTPA-hEGF, 250 ng/mL, was approximately 10-fold more cytotoxic than unlabeled DTPA-hEGF (SF, 6.1% ± 1.9% vs. 60.6% ± 9.9%, respectively; $P < 0.01$). The SF of cells exposed to DTPA-hEGF (250 ng/mL) plus gefitinib (1 μM) did not differ significantly from the SF of cells exposed to 1 μM gefitinib alone (39.9% ± 7.4% vs. 40.3% ± 6.1%, respectively; $P = 0.5$).

DISCUSSION

^{111}In-DTPA-hEGF is rapidly internalized after binding to the EGFR, and a proportion (5%–10%) translocates to the cell nucleus, where the radionuclide comes in close
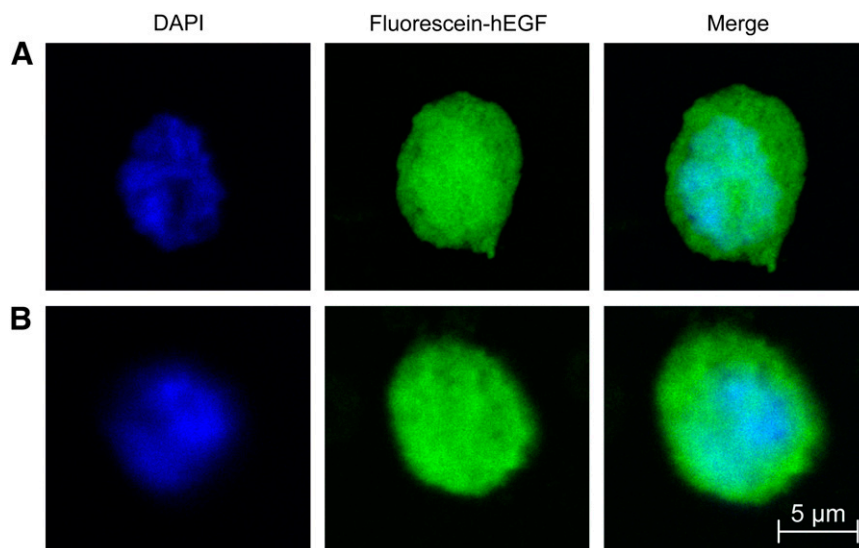
| DAPI | Fluorescein-hEGF | Merge |

FIGURE 2. Visualization of nuclear fluorescein-labeled-hEGF in presence of gefitinib using confocal microscopy. (A) MDA-MB-468 cells treated with fluorescein-hEGF for 1 h at 37°C. (B) MDA-MB-468 cells pretreated with gefitinib (1 μM) for 3 h followed by fluorescein-hEGF and gefitinib for 1 h at 37°C. Cells were also incubated with DAPI to visualize the cell nucleus. Images represent a 1-μm slice through center of cell. Fluorescein-hEGF was observed in the nucleus in absence and presence of 1 μM gefitinib.

proximity to chromosomal DNA (*14*). [111]In emits Auger electrons that can cause lethal DNA damage. Microdosimetry models of Auger electron–emitting radioisotopes in mammalian cells predict that the radiation-absorbed dose to the cell nucleus is 20- to 35-fold greater when ^{111}In is localized in the nucleus compared with when it is localized at the cell membrane (*22*). This prediction is based on the observation that >99% of the Auger electrons emitted by ^{111}In have very low energies (<3 keV) and a range of <1 μm in tissues (*15*). The lethality of Auger electron–emitting radiopharmaceuticals such as ^{111}In-DTPA-hEGF toward cancer cells is therefore likely to be highly dependent on their ability to translocate to the cell nucleus. Pharmacologic strategies that increase the proportion of ^{111}In-DTPA-hEGF that localizes in the nucleus would thus be expected to amplify its cytotoxicity against EGFR-overexpressing cancer cells. It has been shown that EGFR TKIs can increase the cellular uptake of radiolabeled EGF (*18,19*), suggesting that combining ^{111}In-DTPA-hEGF with gefitinib might increase its potency. It has previously been reported that ^{111}In-DTPA-hEGF is only cytotoxic to cells that express moderate to high levels of EGFR. The human breast cancer cell line MCF-7, which

expresses approximately 1×10^4 receptors per cell, was relatively resistant to cell killing by ^{111}In-DTPA-hEGF, both in vitro and in vivo, compared with the MDA-MB-468 cell line, which expresses approximately 1×10^6 EGFRs per cell (*14,17*). Therefore, the ^{111}In-DTPA-hEGF–responsive cell line MDA-MB-468 was selected for this initial investigation of the effect of combining ^{111}In-DTPA-hEGF with EGFR inhibition.

Gefitinib would be expected to enhance the cytotoxicity of ^{111}In-DTPA-hEGF only if inhibition of EGFR phosphorylation does not significantly impede the internalization and nuclear translocation of ^{111}In-DTPA-hEGF. Several investigators have reported that EGFR kinase activation is required for ligand-induced internalization of the receptor (*23,24*). In one study, treatment of NIH3T3 cells expressing EGFR with the TKI PD158780 reduced the internalization rate of the receptor by 90% (*24*). Conversely, in a recent publication, Wang et al. showed that elimination of EGFR kinase activation by mutation or chemical inhibition did not abolish EGFR internalization. Instead, it was shown that inhibition of EGFR dimerization, by deletion of the dimerization loop in domain II, inhibited EGF-dependent EGFR

TABLE 1
Effect of Gefitinib on Binding, Internalization, and Nuclear Localization of ^{111}In-DTPA-hEGF in MDA-MB-468 Human Breast Cancer Cells

Treatment	Proportion (%)		Proportion of cell-bound ^{111}In-DTPA-hEGF (%)	
	Radioactivity bound to cells	Cell-bound radioactivity internalized by cells	Radioactivity within cytoplasm	Radioactivity within nucleus
^{111}In-DTPA-hEGF	54.7 ± 8.6	76.9 ± 5.9	62.3 ± 9.5	14.6 ± 4.0
^{111}In-DTPA-hEGF + gefitinib	58.1 ± 2.8	81.1 ± 1.0	55.0 ± 6.2	26.0 ± 5.5*

*$P < 0.05$.
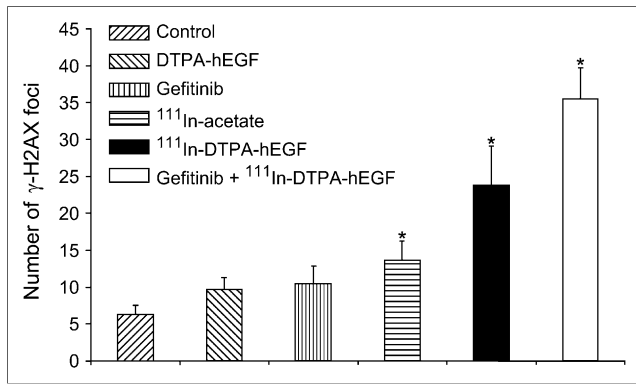Data are expressed as mean ± SD of 3 experiments.

FIGURE 3. Effect of gefitinib and ^{111}In-DTPA-hEGF on induction of γ-H2AX foci in MDA-MB-468 cells. γ-H2AX assay was performed after exposure of MDA-MB-468 cells to DTPA-hEGF (250 ng/mL), gefitinib (1 μM), ^{111}In-acetate (1.5 MBq/mL), ^{111}In-DTPA-hEGF (250 ng/mL, 1.5 MBq/mL), gefitinib (1 μM) plus ^{111}In-DTPA-hEGF (250 ng/mL, 1.5 MBq/mL), or DMEM alone (control) for 20 h. Optical sections (1.2 μm) through the cells were obtained using a confocal microscope and were processed using ImageJ (U.S. National Institutes of Health). Error bars represent SEM number of γ-H2AX foci from 3 separate experiments. Thirty cells were counted to generate each data point for each experiment. *$P < 0.05$ (compared with control).

internalization (25). The apparently contradictory information regarding the need for EGFR phosphorylation in ligand-dependent EGFR internalization could be explained by the existence of redundant pathways of EGFR internalization that may require receptor phosphorylation. It is possible that the dependence of EGFR internalization on EGFR phosphorylation may vary in a cell-type–specific manner (26).

Prevention of EGFR activation through the use of gefitinib did not diminish the internalization and nuclear translocation of fluorescein-labeled hEGF (Fig. 2) or of ^{111}In-DTPA-hEGF in MDA-MB-468 cells (Table 1). Rather, the proportion of radioactivity localizing in the nucleus was 1.8-fold greater in MDA-MB-468 cells treated with the combination of ^{111}In-DTPA-hEGF (5 ng/mL, 3.7 MBq/μg) and gefitinib (1 μM) compared with ^{111}In-DTPA-hEGF alone. Although EGF–EGFR trafficking is incompletely understood, it is apparent that after cellular uptake into clathrin-coated pits, the ligand–receptor complex is internalized into endosomes. From early endosomes, EGFR either is sorted into the late endosome and then sent to the lysosome for degradation or is recycled back to the cell surface. Recent evidence also suggests that ligand-dependent translocation of EGFR to the nucleus can occur (27). The route through which EGFR reaches the nucleus is unclear (28), although a putative nuclear localizing sequence has been identified in the cytoplasmic domain and EGFR has been shown to associate with importins α_1/β_1 and exportin CRM1 (29). This suggests that nuclear uptake of EGFR is mediated by the nuclear transport receptors and the nuclear pore complex. Sorting of EGFR to the lysosome requires phosphorylation of EGFR at Tyr-1045. Phosphorylation at this site is necessary to recruit c-Cbl, which ubiquitinates
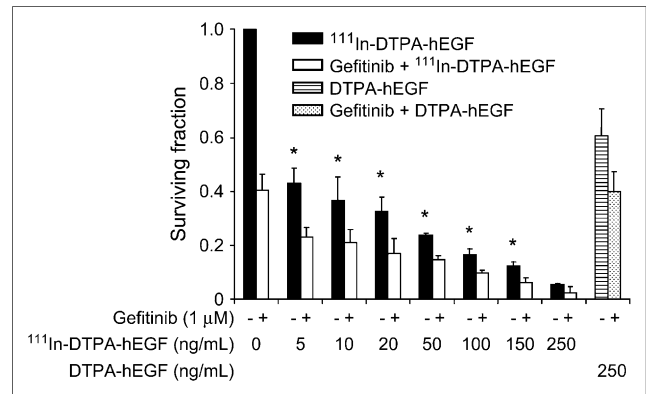

FIGURE 4. Gefitinib enhances ^{111}In-DTPA-hEGF–mediated cytotoxicity. Clonogenic assay was performed using MDA-MB-468 cells treated with increasing concentrations of ^{111}In-DTPA-hEGF (5–250 ng/mL, 6 MBq/μg) for 24 h at 37°C (black bars) or pretreated with gefitinib (1 μM) for 3 h followed by treatment with a range of concentrations of ^{111}In-DTPA-hEGF plus gefitinib (1 μM) for 24 h at 37°C (white bars). At each concentration of ^{111}In-DTPA-hEGF tested, addition of gefitinib resulted in enhanced cytotoxicity. The SF of cells exposed to DTPA-hEGF (250 ng/mL) in the absence or presence of gefitinib (1 μM) was also measured (lined and speckled bars, respectively). ^{111}In-DTPA-hEGF (250 ng/mL) was ~10-fold more cytotoxic than unlabeled DTPA-hEGF (SF, 6.1% $\pm$ 1.9% vs. 60.6% $\pm$ 9.9%, respectively; $P < 0.01$). The SF of cells exposed to DTPA-hEGF (250 ng/mL) plus gefitinib (1 μM) was not statistically significant from the SF of cells exposed to 1 μM gefitinib alone (39.9% $\pm$ 7.4% vs. 40.3% $\pm$ 6.1%, respectively; $P = 0.5$). Error bars represent SD of the mean SF calculated from 3 separate experiments. *$P < 0.05$ (compared with control).

EGFR, directing it to the lysosome for degradation (30). Thus, one possible mechanism for increased nuclear uptake of ^{111}In-DTPA-hEGF in the presence of gefitinib is that blocked phosphorylation of EGFR enables the ligand–receptor complex to escape lysosome-mediated degradation. This could allow a proportionately greater amount of the receptor to accumulate in the cell nucleus or to be recycled back to the cell membrane. It is also important to note that the effect of ^{111}In-DTPA-hEGF on EGFR activation and trafficking is likely to be distinct from that of the naked ligand, EGF—because ionizing radiation and other sources of oxyradicals lead to aberrant phosphorylation of the receptor (31). In these circumstances EGFR does not undergo ubiquitination or endocytosis but may traffick to perinuclear and nuclear compartments (32,33).

Overall, the results presented in this article suggest that the enhanced cytotoxicity observed with concomitant ^{111}In-DTPA-hEGF and gefitinib treatment is at least partially due to an increase in the nuclear translocation of the radiopharmaceutical. However, there are likely to be other factors that contribute to the increased lethality of ^{111}In-DTPA-hEGF in the presence of gefitinib compared with ^{111}In-DTPA-hEGF alone. It has been reported that EGFR is involved in the activation and regulation of DNA-dependent kinase (DNA-PK), which participates in the nonhomologous end-joining (NHEJ) DNA repair pathway (33,34). As

a result, NHEJ may be less active in EGFR inhibitor–treated cells. Friedmann et al. have shown that exposure of the breast cancer cell line MCF-7 to gefitinib leads to a reduction in nuclear DNA-PK, suppression of DNA-PK activity, and sensitization to DNA damage by cisplatin (35). DNA-PK is known to play a central role in the repair of radiation DNA damage. Therefore, it is possible that the increase in γ-H2AX foci and lower SF that were observed in cells treated with ^{111}In-DTPA-hEGF in the presence of gefitinib compared with ^{111}In-DTPA-hEGF alone may be the result of gefitinib-mediated inhibition of DNA-PK activity.

Small-molecule TKIs have been shown to cause cell cycle arrest in the G_0/G_1 phase and to reduce the percentage of cells in the radiation-resistant S-phase fraction in malignant cell lines (36). Depending on the duration of cell cycle arrest caused by TKIs and the effect of ^{111}In-DTPA-hEGF itself on cell cycle kinetics, it is possible that partial synchronization of cells by a TKI might render them more susceptible to the cytotoxicity of ^{111}In-DTPA-hEGF, although this has yet to be confirmed experimentally.

The induction of DNA damage by ^{111}In-DTPA-hEGF with and without gefitinib was evaluated by counting the number of γ-H2AX foci formed at the sites of DNA-dsbs. Sedelnikova et al. have reported a positive correlation between the number of γ-H2AX foci and clonogenic survival in cells transfected with ^{125}I-triplex-forming oligonucleotides, suggesting that the γ-H2AX assay is a useful marker of the cytotoxic effects of Auger electron–emitting DNA-targeting agents (37). It was found that the average number of γ-H2AX foci per nucleus increased 1.5-fold when ^{111}In-DTPA-hEGF was combined with gefitinib in comparison with cells incubated with the radiopharmaceutical alone (Fig. 3). Also, ^{111}In-DTPA-hEGF resulted in a significantly greater number of foci than ^{111}In-acetate (23.8 ± 5.2 vs. 13.6 ± 2.5 foci, respectively; $P < 0.05$). In contrast to Auger electrons, which have a subcellular range, the 171- and 245-keV γ-photons that ^{111}In also emits have a range that is much greater than a cell diameter. Because ^{111}In-acetate is not specifically taken up by the cells, the low level of DNA damage that it causes is likely due to γ-irradiation from extracellular ^{111}In-acetate or to Auger electrons emitted by a limited amount of intracellular [111]In. Taken together, these results suggest that it is the Auger electron emissions that cause most of the DNA damage caused by ^{111}In-DTPA-hEGF and that specific binding of the radiopharmaceutical to EGFR is a prerequisite for the significant induction of DNA-dsbs. The increased level of DNA damage observed when ^{111}In-DTPA-hEGF was combined with gefitinib was reflected in lower clonogenic survival of cells exposed to both agents (Fig. 4). Unlabeled DTPA-hEGF at high concentration (250 ng/mL) resulted in a modest reduction in SF, which is consistent with the reported observation that high concentrations of EGF are inhibitory to the growth of MDA-MB-468 cells (16). The same concentration of ^{111}In-DTPA-hEGF was approximately 10-fold more cytotoxic than unla-beled DTPA-hEGF (SF: 6.1% ± 1.9% vs. 60.6% ± 9.9%, respectively; $P < 0.01$). The SF of cells exposed to DTPA-hEGF plus gefitinib did not differ significantly from the SF of cells exposed to gefitinib alone. These results indicate that the deleterious effect of ^{111}In-DTPA-hEGF plus gefitinib is due to Auger electron radiation and not simply to an increase in nuclear uptake of DTPA-hEGF after gefitinib treatment.

It was calculated that, for the concentration of ^{111}In-DTPA-hEGF used in the cellular fractionation experiments described in this article (5 ng/mL, 3.7 MBq/µg), approximately 12% of EGFs would be occupied. If it is assumed that the cellular distribution is similar under receptor saturation conditions, then—based on the cellular distribution data that were obtained for ^{111}In-DTPA-hEGF alone and in combination with gefitinib (Table 1)—the radiation dose delivered to the entire cell, and specifically to the cell nucleus under both treatment conditions, can be calculated using a microdosimetry model. Goddu et al. tabulated S values (absorbed dose per unit of cumulated activity) for cells and nuclei of various sizes and for several isotopes, including [111]In (22). Using these S values and assuming a cell diameter of 10 µm and a nuclear diameter of 6 µm, each MDA-MB-468 cell treated to receptor saturation with ^{111}In-DTPA-hEGF would receive 20.2 Gy to the nucleus. Nuclear ^{111}In-DTPA-hEGF accounts for 16.0 Gy of this total (Table 2). Because radioactivity localized to the nucleus accounts for 80% of the absorbed-radiation dose to the nucleus (22), even a modest increase in nuclear ^{111}In-DTPA-hEGF would result in a significant increase in the absorbed-radiation dose to DNA. It is estimated that the addition of gefitinib to ^{111}In-DTPA-hEGF resulted in a total absorbed dose of 32.3 Gy to the cell nucleus, of which 28.6 Gy were due to ^{111}In-DTPA-hEGF in the nucleus (Table 2). Thus, the 1.8-fold increase in the amount of radioactivity in the nucleus associated with gefitinib treatment results in an additional 12.2-Gy absorbed dose to the nucleus. It is possible that the absorbed-radiation doses shown in Table 2 are overestimated, as the method used to obtain them accounts for radioactive decay but not for biologic clearance of radioactivity from the cell. However, it has been shown previously that nuclear accumulation of ^{111}In-DTPA-hEGF increases for up to 24 h in MDA-MB-468 cells. Given that cells were exposed to ^{111}In-DTPA-hEGF for 24 h in this study, the effect of egress of radioactivity on the absorbed-dose calculation is likely to be small (14).

The current study shows that, in a commonly used model of EGFR-positive human breast cancer, the efficacy of targeted Auger electron radiotherapy can be improved by a pharmacologic intervention that increases nuclear uptake of the agent. The use of combination treatment with a TKI is one way to increase the uptake of ^{111}In-DTPA-hEGF and increase the chance of successful eradication of malignant cells. The concentration of gefitinib used in the experiments described in this report (1 µM) is within the range of human steady-state plasma concentrations (0.4–1.2 µM) resulting from clinically relevant doses of the drug (250–500 mg

TABLE 2
Effect of Gefitinib on Radiation-Absorbed Dose to Cell Nucleus from ^{111}In-DTPA-hEGF Localized at Cell Membrane, Cytoplasm, or Nucleus of MDA-MB-468 EGFR-Overexpressing Human Breast Cancer Cells*

Treatment	Cell compartment	$\bar{A}$ (Bq × s)[†]	S ([Gy/Bq × s] × 10⁻⁴)	Radiation dose to nucleus $\bar{D}$, (Gy)[‡]
^{111}In-DTPA-hEGF	Membrane	4,240	1.78	0.75
	Cytoplasm	11,307	3.18	3.4
	Nucleus	2,651	60.3	16.0
	Total			20.15
^{111}In-DTPA-hEGF + gefitinib	Membrane	3,432	1.78	0.61
	Cytoplasm	9,894	3.18	3.15
	Nucleus	4,735	60.3	28.55
	Total			32.31

*Radiation-absorbed dose ($\bar{D}$) to cell nucleus was estimated using cellular radiation dosimetry model of Goddu et al. (22): $\bar{D} = \bar{A} \times S$, where S is radiation-absorbed dose in nucleus (Gy) per unit of cumulated radioactivity in source compartment, $\bar{A}$ (Bq × s).

[†]$\bar{A} = A_0/\lambda$, where A_0 is amount of radioactivity localized in the compartment at time 0, and λ is radioactive decay constant for [111]In (2.83×10^{-6}/s). Rapid localization of ^{111}In-DTPA-hEGF in the compartment and rate of elimination corresponding to radioactive decay of radionuclide ^{111}In are assumed.

[‡]Based on each MDA-MB-468 cell having a diameter of 10 μm and a nuclear diameter of 6 μm. Assumes targeting of a single cell with ^{111}In-DTPA-hEGF to receptor saturation. At receptor saturation, ~48 mBq ^{111}In-DTPA-hEGF would be bound to each MDA-MB-468 cell at a specific activity of 3.7 MBq/μg.

daily) (38). This suggests that the enhancement of the cytotoxicity of ^{111}In-DTPA-hEGF when combined with gefitinib would be achievable in the clinical setting. Gefitinib is well tolerated at a dose of up to 600 mg/d (38), so it may be possible to further enhance the cytotoxicity of ^{111}In-DTPA-hEGF by increasing the dose of gefitinib with which it is combined, although this has yet to be tested.

It is possible that pharmacologic interventions that alter endosomal trafficking or nuclear transport might further promote nuclear uptake and, thus, efficacy of ^{111}In-DTPA-hEGF. One possible strategy to increase nuclear uptake might involve the addition of a nuclear localization sequence (NLS) to radiopharmaceuticals. A recent study reported a higher internalization rate, prolonged cellular retention, and significantly higher nuclear uptake when the NLS of the simian virus 40 large T-antigen was conjugated to ^{111}In-DOTA-octreotide compared with the unmodified drug, ^{111}In-DOTA-Tyr[3]-octreotide (39). Similarly, we have recently reported increased nuclear localization and decreased clonogenic survival in leukemia cells exposed to an anti-CD33 monoclonal antibody, HuM195, radiolabeled with ^{111}In and modified with nuclear-localization-sequence peptides of the simian virus 40 large T-antigen (40).

CONCLUSION

Gefitinib increases the accumulation of ^{111}In-DTPA-hEGF in the nucleus, leading to an increase in DNA double-strand breaks and cell death. Because the localization of ^{111}In-DTPA-hEGF and other Auger electron–emitting radiopharmaceuticals controls lethality, manipulating the nuclear translocation pathway to amplify the amount of short-range radioactivity accumulating in the nucleus is an effective means by which to enhance cytotoxicity. A greater knowledge of the nuclear translocation pathway of ^{111}In-DTPA-hEGF may suggest other mechanisms for enhancing the nuclear uptake of ^{111}In-DTPA-hEGF in the future.

REFERENCES

1. Yarden Y, Sliwkowski MX. Untangling the ErbB signalling network. *Nat Rev Mol Cell Biol.* 2001;2:127–137.
2. Fox SB, Harris AL. The epidermal growth factor receptor in breast cancer. *J Mammary Gland Biol Neoplasia.* 1997;2:131–141.
3. Nyati MK, Morgan MA, Feng FY, Lawrence TS. Integration of EGFR inhibitors with radiochemotherapy. *Nat Rev Cancer.* 2006;6:876–885.
4. Herbst RS, Giaccone G, Schiller JH, et al. Gefitinib in combination with paclitaxel and carboplatin in advanced non-small-cell lung cancer: a phase III trial—INTACT 2. *J Clin Oncol.* 2004;22:785–794.
5. Blackhall F, Ranson M, Thatcher N. Where next for gefitinib in patients with lung cancer? *Lancet Oncol.* 2006;7:499–507.
6. von Minckwitz G, Jonat W, Fasching P, et al. A multicentre phase II study on gefitinib in taxane- and anthracycline-pretreated metastatic breast cancer. *Breast Cancer Res Treat.* 2005;89:165–172.
7. ECOG E1100: a phase II trial of trastuzumab and gefitinib in patients with metastatic breast cancer that overexpress HER2/neu (erbB-2). *Clin Adv Hematol Oncol.* 2003;1:237.
8. Ciardiello F, Troiani T, Caputo F, et al. Phase II study of gefitinib in combination with docetaxel as first-line therapy in metastatic breast cancer. *Br J Cancer.* 2006;94:1604–1609.
9. Okubo S, Kurebayashi J, Otsuki T, Yamamoto Y, Tanaka K, Sonoo H. Additive antitumour effect of the epidermal growth factor receptor tyrosine kinase

inhibitor gefitinib (Iressa, ZD1839) and the antioestrogen fulvestrant (Faslodex, ICI 182,780) in breast cancer cells. *Br J Cancer.* 2004;90:236–244.

10. Akimoto T, Hunter NR, Buchmiller L, Mason K, Ang KK, Milas L. Inverse relationship between epidermal growth factor receptor expression and radio-curability of murine carcinomas. *Clin Cancer Res.* 1999;5:2884–2890.

11. Harari PM, Huang SM. Head and neck cancer as a clinical model for molecular targeting of therapy: combining EGFR blockade with radiation. *Int J Radiat Oncol Biol Phys.* 2001;49:427–433.

12. Bonner JA, Harari PM, Giralt J, et al. Radiotherapy plus cetuximab for squamous-cell carcinoma of the head and neck. *N Engl J Med.* 2006;354:567–578.

13. Baumann M, Krause M. Targeting the epidermal growth factor receptor in radio-therapy: radiobiological mechanisms, preclinical and clinical results. *Radiother Oncol.* 2004;72:257–266.

14. Reilly RM, Kiarash R, Cameron RG, et al. ^{111}In-Labeled EGF is selectively radiotoxic to human breast cancer cells overexpressing EGFR. *J Nucl Med.* 2000;41:429–438.

15. Howell RW. Radiation spectra for Auger-electron emitting radionuclides: report no. 2 of AAPM Nuclear Medicine Task Group no. 6. *Med Phys.* 1992;19:1371–1383.

16. Chen P, Mrkobrada M, Vallis KA, et al. Comparative antiproliferative effects of ^{111}In-DTPA-hEGF, chemotherapeutic agents and gamma-radiation on EGFR-positive breast cancer cells. *Nucl Med Biol.* 2002;29:693–699.

17. Chen P, Cameron R, Wang J, Vallis KA, Reilly RM. Antitumor effects and normal tissue toxicity of ^{111}In-labeled epidermal growth factor administered to athymic mice bearing epidermal growth factor receptor-positive human breast cancer xenografts. *J Nucl Med.* 2003;44:1469–1478.

18. Lichtner RB, Menrad A, Sommer A, Klar U, Schneider MR. Signaling-inactive epidermal growth factor receptor/ligand complexes in intact carcinoma cells by quinazoline tyrosine kinase inhibitors. *Cancer Res.* 2001;61:5790–5795.

19. Sundberg AL, Almqvist Y, Orlova A, et al. Combined effect of gefitinib ('Iressa', ZD1839) and targeted radiotherapy with [211]At-EGF. *Eur J Nucl Med Mol Imaging.* 2003;30:1348–1356.

20. Reilly RM, Gariepy J. Factors influencing the sensitivity of tumor imaging with a receptor-binding radiopharmaceutical. *J Nucl Med.* 1998;39:1036–1043.

21. Haigler H, Ash JF, Singer SJ, Cohen S. Visualization by fluorescence of the binding and internalization of epidermal growth factor in human carcinoma cells A-431. *Proc Natl Acad Sci USA.* 1978;75:3317–3321.

22. Goddu SM, Howell RW, Rao DV. Cellular dosimetry: absorbed fractions for monoenergetic electron and alpha particle sources and S-values for radionuclides uniformly distributed in different cell compartments. *J Nucl Med.* 1994;35:303–316.

23. Lamaze C, Schmid SL. Recruitment of epidermal growth factor receptors into coated pits requires their activated tyrosine kinase. *J Cell Biol.* 1995;129:47–54.

24. Sorkina T, Huang F, Beguinot L, Sorkin A. Effect of tyrosine kinase inhibitors on clathrin-coated pit recruitment and internalization of epidermal growth factor receptor. *J Biol Chem.* 2002;277:27433–27441.

25. Wang Q, Villeneuve G, Wang Z. Control of epidermal growth factor receptor endocytosis by receptor dimerization, rather than receptor kinase activation. *EMBO Rep.* 2005;6:942–948.

26. Jiang X, Huang F, Marusyk A, Sorkin A. Grb2 regulates internalization of EGF receptors through clathrin-coated pits. *Mol Biol Cell.* 2003;14:858–870.

27. Lin SY, Makino K, Xia W, et al. Nuclear localization of EGF receptor and its potential new role as a transcription factor. *Nat Cell Biol.* 2001;3:802–808.

28. Carpenter G. Nuclear localization and possible functions of receptor tyrosine kinases. *Curr Opin Cell Biol.* 2003;15:143–148.

29. Lo HW, Ali-Seyed M, Wu Y, Bartholomeusz G, Hsu SC, Hung MC. Nuclear-cytoplasmic transport of EGFR involves receptor endocytosis, importin beta1 and CRM1. *J Cell Biochem.* 2006;98:1570–1583.

30. Grovdal LM, Stang E, Sorkin A, Madshus IH. Direct interaction of Cbl with pTyr 1045 of the EGF receptor (EGFR) is required to sort the EGFR to lysosomes for degradation. *Exp Cell Res.* 2004;300:388–395.

31. Ravid T, Sweeney C, Gee P, Carraway KL III, Goldkorn T. Epidermal growth factor receptor activation under oxidative stress fails to promote c-Cbl mediated down-regulation. *J Biol Chem.* 2002;277:31214–31219.

32. Khan EM, Heidinger JM, Levy M, Lisanti MP, Ravid T, Goldkorn T. Epidermal growth factor receptor exposed to oxidative stress undergoes Src- and caveolin-1-dependent perinuclear trafficking. *J Biol Chem.* 2006;281:14486–14493.

33. Dittmann K, Mayer C, Fehrenbacher B, et al. Radiation-induced epidermal growth factor receptor nuclear import is linked to activation of DNA-dependent protein kinase. *J Biol Chem.* 2005;280:31182–31189.

34. Bandyopadhyay D, Mandal M, Adam L, Mendelsohn J, Kumar R. Physical interaction between epidermal growth factor receptor and DNA-dependent protein kinase in mammalian cells. *J Biol Chem.* 1998;273:1568–1573.

35. Friedmann BJ, Caplin M, Savic B, et al. Interaction of the epidermal growth factor receptor and the DNA-dependent protein kinase pathway following gefitinib treatment. *Mol Cancer Ther.* 2006;5:209–218.

36. Chinnaiyan P, Huang S, Vallabhaneni G, et al. Mechanisms of enhanced radiation response following epidermal growth factor receptor signaling inhibition by erlotinib (Tarceva). *Cancer Res.* 2005;65:3328–3335.

37. Sedelnikova OA, Panyutin IV, Neumann RD, Bonner WM, Panyutin IG. Assessment of DNA damage produced by ^{125}I-triplex-forming oligonucleotides in cells. *Int J Radiat Biol.* 2004;80:927–931.

38. Baselga J, Rischin D, Ranson M, et al. Phase I safety, pharmacokinetic, and pharmacodynamic trial of ZD1839, a selective oral epidermal growth factor receptor tyrosine kinase inhibitor, in patients with five selected solid tumor types. *J Clin Oncol.* 2002;20:4292–4302.

39. Ginj M, Hinni K, Tschumi S, Schulz S, Maecke HR. Trifunctional somatostatin-based derivatives designed for targeted radiotherapy using Auger electron emitters. *J Nucl Med.* 2005;46:2097–2103.

40. Chen P, Wang J, Hope K, et al. Nuclear localizing sequences promote nuclear translocation and enhance the radiotoxicity of the anti-CD33 monoclonal antibody HuM195 labeled with ^{111}In in human myeloid leukemia cells. *J Nucl Med.* 2006;47:827–836.